INVESTIGATIONS ON THE ENERGY INFLUX AT PLASMA SURFACE PROCESSES*

H. Kersten, D. Rohde, H. Deutsch, R. Hippler
Department of Physics, University of Greifswald, Domstrasse 10a, D-17487 Greifswald, Germany

W.W. Stoffels, E. Stoffels, G.M.W. Kroesen
Department of Physics, Technical University Eindhoven, P.O.Box 513, 5600MB Eindhoven, The Netherlands

J. Berndt
Institute for Experimental Physics II, Ruhr-University Bochum, Building NB5/131, D-44780 Bochum, Germany

Received 28 June 2000, accepted 30 June 2000

A summary is given of different elementary processes influencing the thermal balance and energetic conditions of substrate surfaces during plasma processing. The discussed mechanisms include heat radiation, kinetic and potential energy of charged particles and neutrals as well as enthalpy of involved chemical surface reactions. The energy and momentum of particles originating from the plasma or electrodes, respectively, influence via energy flux density (energetic aspect) and substrate temperature (thermal aspect) the surface properties of the treated substrates. For a few examples as magnetron sputtering of a-C:H films, sputter deposition of aluminum on micro-particles, and atomic nitrogen recombination in an ECR plasma the energetic balance of substrates during plasma processing are presented.

PACS: 52.75.Rx, 81.15.Gh, 07.07.Df, 07.20.Dt

1 Introduction

At present, plasma processing of materials is one of the fastest growing branches in plasma physics and has got a prominent position in the rather new field of applied surface science. In particular, plasma-wall interactions are of great importance in a large variety of applications of low-temperature, low-pressure plasmas in such fields as etching, deposition and surface modification of thin films. In these processes the thermal and energetic conditions at the substrate surface play a dominant role.

In detail, low temperature plasma processing of solid surfaces is mainly affected by the following quantities:

*Presented at the Workshop on Solid State Surfaces and Interfaces II, Bratislava, Slovakia, June 20 – 22, 2000.

- energy per incoming particle (E), which is related to energy transfer,
- particle flux density to the substrate (j), which is related to momentum transfer,
- energy flux density ($J = jE$), representing a key parameter for the energetic conditions at the surface, and
- temperature of the substrate surface (T_S), which results from the inner parameters (E, j) mentioned above and which reflects the thermal balance at the surface as a macroscopic quantity.

The surface temperature T_S, which can also be influenced by external heating, effects elementary processes like adsorption, desorption, and diffusion as well as chemical reactions (chemical sputtering, surface film reaction [1-4].

On the other hand, especially in the case of thin film deposition, the structure and morphology as well as the stoichiometry of the film depend strongly on the energetic conditions (J) at the surface, see for example [1,5-10]. The surface diffusion of adsorbed atoms can be enhanced, which results in a rearrangement of deposited atoms [11,12]. Bombardment of a growing film with low- energy ions results in a modification of its properties, see for example [13].

It should be emphasized, that in addition to external heating the surface temperature T_S is largely influenced by the energy fluxes resulting from energetic particle bombardment, chemical surface reactions and heat radiation [14]-[16]. By a suitable variation of the experimental conditions the different contributions to the substrate heating can be separated and studied independently.

Besides radiation from the environment (plasma, walls), the energy influx consists of kinetic energy and potential energy of the incoming particles. The distribution of the several energetic contributions depends on the discharge conditions and the substrate potential. Therefore, the experimental investigation of plasma-wall interaction due to energy transfer in technological plasma processing requires sophisticated measurements [17,18].

In the first part of the paper we will attempt to give a short description of relevant channels for substrate heating and surface modification, respectively, and their transfer mechanisms. In the following section, various methods for an experimental determination of energy fluxes are described. Finally, implementations of the models for a few specific, experimentally studied plasma-substrate systems will be described.

2 Energy balance at the substrate surface

2.1 Contributions to the integral energy influx

When a plasma acts on a solid surface the surfaces is heated due to energy transfer which can be described by a balance of the involved energy fluxes. In general, the total power input Qin at the substrate surface is the surface integral over the sum of different contributions J (energy flux per time and area):

$$Q_{in} = \int (J_{rad} + J_{ch} + J_n + J_{ads} + J_{react} + J_{ext}) dA. \tag{1}$$

J_{rad} is the heat radiation towards the surface, J_{ch} the power transferred by charge carriers (electrons and ions), and J_n is the contribution of neutral species of the background gas and the

neutral particles contributing to the film growth. The latter terms in Eq. (1) are energy released by adsorption or condensation (J_{ads}) and the reaction energy of exothermic processes including molecular surface recombination (J_{react}). Additionally, also power input by external sources (J_{ext}) influences the thermal balance of the substrate.

In the following the different contributions to the integral heat influx during low-temperature plasma processing will be described shortly.

Heat Radiation (J_{rad})

Radiative energy sources in plasma processing might be the surrounding surfaces (e.g. reactore walls, enclosure), hot material sources (e.g. crucibles) and the gas/plasma radiation itself. Hence, heat radiation J_{rad} becomes important in high temperature plasmas and/or if the temperature of the reactor walls is high due to external heating as for example in plasma enhanced chemical vapour deposition (PECVD). Also in evaporation processes where molten materials are employed for thin film deposition (e.g. electron beam evaporation, hollow cathode arc evaporation) the heat radiation of the crucible can be an essential contribution to the global energy balance of the substrate treated.

In most cases it is sufficient to take into account the simplification of the Boltzmann formula for heat transfer by radiation:

$$J_{rad} = \sigma(\epsilon T_{rad}^4 - \epsilon_S T_S^4). \tag{2}$$

Here ϵ is the spectral emittance of the radiation source at temperature T_{rad} and ϵ_S represents the spectral emmitance of the substrate surface at temperature T_S while σ denotes the Stefan-Boltzmann constant.

Usually, the contribution of heat radiation from hot surfaces in a common low-temperature plasma reactor is small, but in some applications in combination with CVD or arc evaporation it can amount up to several tens of per cent. Besides radiation from the enclosure walls or evaporation sources there are also radiative contributions from excited species of the plasma in form of photons ranging from IR to UV. However, it is very difficult to measure and to calibrate this contribution on the integral energy flux.

Energy influx by charge carriers (J_{ch})

For many applications, non-isothermal low pressure discharges play an important role in plasma processing. In those discharges, the most efficient channel of energy transfer is due to charge carriers, which get their directed kinetic energy in every case by acceleration in the sheath in front of a surface.

The energy of ions striking the substrate is the sum of potential $E_{i,pot}$ and kinetic energy $E_{i,kin}$. The potential neutralization energy of ions on surfaces is caused by long-range interactions and is accompanied by the emission of secondary electrons. Then $E_{i,pot}$ is given to

$$E_{i,pot} = E_i - \Phi - \gamma_i(\Phi + E_{i,kin}) \tag{3}$$

(E_i: ionization potential of the incident ion, Φ: work function, γ_i: yield of secondary electrons, $E_{i,kin}$: mean kinetic energy of incident ion). Data for E_i, Φ and γ_i, respectively, may be taken from the literature [19,20]. For semiconductors the yield of secondary electron emission is one order of magnitude smaller than for metals [19]. The work function Φ for metals and semiconductors is in order of ~ 5 eV.

In systems where the heat flux to the surface is dominated by ion bombardment (e.g. in planar RF reactors) the contribution of the potential energy term [Eq. (3)] can be very substantial (several tens of percent) for low kinetic energies [21].

In addition to potential energy, ions transfer a part of their kinetic energy when striking a surface. In general, the mean kinetic ion energy $E_{i,kin}$ is determined by the ion energy distribution function (IEDF). The energy distribution of the ions arriving at the substrate is affected by the pressure which influences the collisions in the sheath in front of the substrate and by the instantaneous, local electric field. These effects may lead to a broadening, to a shift, and to various shapes of the IEDF. The maximum ion energy is determined by the free fall energy $e_0 V_{sh}$, where V_{sh} is the potential drop across the sheath in front of the substrate which corresponds to the sum of the plasma potential V_{pl} and the substrate potential V_S:

$$V_{sh} = V_{bias} = V_{pl} + V_S. \tag{4}$$

The value of the sheath potential is essentially determined by the internal plasma parameter as electron density and the energy distribution of electrons and ions in the plasma.

In addition to the directed kinetic energy of the ions which originates for positive ions from acceleration in the electrical field in front of the substrate, they receive thermal energy kT_i, too (k: Boltzmann constant, T_i: ion temperature). As mentioned above, the directed kinetic energy can be assumed in most cases to be approximately equal to the sheath potential. Hence, the total kinetic energy of positive ions equals

$$E_{i,kin} = \frac{3}{2} kT_i + e_0 V_{bias}. \tag{5}$$

The contributions of positive and negative ions as well as of the electrons and the distribution between these striking particles in respect to the energy transfer depends strongly on the substrate bias voltage which consists of the external substrate voltage V_S and the plasma potential V_{pl}, see Eq. (4). For highly negative voltages only the positive ions determine the influence of the charge carriers, whereas electrons and/or negative ions have to be considered in the case of $V_{bias} > 0$.

It should be emphasized again that the simple expression of Eq. (5) is applicable in most cases of plasma processing. However, if the IEDF for the ions near the substrate is much more complex the assumption of $e_0 V_{bias}$ for the kinetic energy fails. By considering this fact one has to integrate over the ion energy distribution function $f(V)$ from zero up to the bias potential V_{bias} in order to obtain the mean kinetic ion energy:

$$E_{i,kin} = \int_0^{V_{bias}} f(V) V \, dV. \tag{6}$$

Furthermore, the thermal energy of the ions (kT_i) can be neglected compared to the directed kinetic energy in non-isothermal plasma process applications because the ions are nearly at room temperature. In high temperature isothermal plasmas and at high pressures this assumption is not valid and the gradient between ion temperature and substrate temperature has to be taken into account for the determination of the energy influx by ions [22].

An exact description of the electron behaviour in a non-isothermal gas discharge requires the knowledge of the electron energy distribution function (EEDF) which can be determined by Langmuir-probe measurements, see for instance [23,24]. In some cases it is possible to model

the EEDF by means of standard distributions, for example Maxwell or Druyvesteyn distribution. Comparing the most common standard distribution functions, there is a significant difference in their high energy tails. In order to reach the substrate surface the electrons have to overcome the bias voltage V_{bias} in front of the substrate. The energy flux J_e due to the plasma electrons arises from the integration over the EEDF from V_{bias} up to infinity which yields for a Maxwellian EEDF:

$$J_e = n_e \sqrt{\frac{kT_e}{2\pi m_e}} \exp\left(-\frac{e_0 V_{bias}}{kT_e}\right) 2kT_e = j_e E_e. \tag{7}$$

By comparison of the terms one can identify the energy of the plasma electrons as:

$$E_e = \int_{V_{bias}}^{\infty} f(E) E \, dE = 2kT_e \tag{8}$$

where the electron flux density of the plasma electrons j_e can be expressed by:

$$j_e = n_e \sqrt{\frac{kT_e}{2\pi m_e}} \exp\left(-\frac{e_0 V_{bias}}{kT_e}\right). \tag{9}$$

An analysis of the charged components of the plasma by using the general equations (2)-(9) listed above will in principle yield the part of surface heating caused by ions and electrons. Although several heat sources act together, e.g. radiation, chemical reactions, neutrals, and charge carriers, it may be possible to separate the contribution of the charge carriers by variation of the bias potential.

Energy influx by neutral species (J_n)

In addition to charge carriers, neutrals of the background gas as well as neutrals of the process itself (e.g. deposition material, etch products, radicals, etc.) interact with the substrates in plasma processing of solid surfaces and, hence, contribute to the thermal power balance. The potential energy of neutral species in a plasma is distributed between vibration, rotation, dissociation and electronically excited states (metastables), while the kinetic energy arises only from the translation. In general, the following components may contribute to the energy transfer by neutrals in commonly used plasma process applications at low pressure:

- heat of adsorption J_{ads} or condensation J_c, respectively,
- excitation energy (vibration, rotation, metastables), J_*
- kinetic energy of sputtered or scattered particles from the cathode, $J_{n,sput}$
- energetic neutrals of the process gas ($J_{n,kin}$) which may originate from charge exchange mechanisms.

The first two components represent the most important transfer channels of potential energy. A short review on the different kinds of potential energy transfer mechanisms of the excitation modes may be found in [25,26].

Energy influx by exothermic chemical reactions (J_{react})
Evidence for substrate heating by exothermic reactions on the processed surface has been reported, for example, with respect to plasma etching of silicon with fluorine containing compounds [27] and during plasma cleaning of contaminated metal surfaces [28]. If the reaction of atoms to product molecules is an exothermic process, which takes place in the presence of a third collision partner, e.g. a solid surface, this process will contribute to substrate heating. The product molecules may desorb at the electronic ground state, but with internal excitation of vibration or rotation. Thus, there is a varying part of the reaction energy transferred between the solid surface and the desorbed molecule. The latter part is used as desorption energy. Concerning the recombination of atoms on a solid surface one has to distinguish between two basic mechanisms: In the case of the Langmuir-Hinshelwood mechanism two adsorbed atoms recombine to a resulting product molecule removing an energy equal to the activation energy of molecular desorption [29]. For the Eley-Rideal mechanism a molecule is generated by gas phase atom impact on an adsorbed atom [30]. A Eley-Rideal-produced molecule may immediately escape or remain physisorbed for a residence time during which it may deposit some part of its energy.

2.2 Energy loss processes

From a general point of view and similar to the energy input, the heat loss Q_{out} of the substrate during plasma processing consist of the following terms:

$$Q_{out} = \int (J_{rad} + J_{ext} + J_{des} + J_{react} + J_{particle}) dA. \tag{10}$$

- energy J_{rad} radiated from the substrate at temperature T_S, which includes contributions of both the front side in direction of the plasma and the back side of the substrate in direction of the holder,
- heat loss J_{ext} by external cooling, i.e. the energy transport by conduction along the substrate holder and by convection of the surrounding gas,
- energy sink J_{des} due to desorption of particles into the gas phase,
- energy J_{react} concerning endothermic chemical reactions at the surface including dissociation,
- energy transport $J_{particle}$ from the substrate due to sputtering of surface atoms and secondary electron emission.

3 Determination of the energy influx

When a solid comes into contact with a plasma, energy transfer takes place. The substrate is heated and, after a certain time, it may reach a thermal equilibrium. This steady state is determined by a balance of energy gain from the plasma processes and energy losses by conduction and radiation [14],[17,31]. The general power balance at the substrate is given by:

$$Q_{in} = \dot{H}_S + Q_{out} \tag{11}$$

where $\dot{H}_S = mc\frac{dT_S}{dt}$ denotes the enthalpy of the substrate and Q_{out} summarizes the heat losses by radiation and thermal conduction by the gas and the substrate. For most substrates thermal

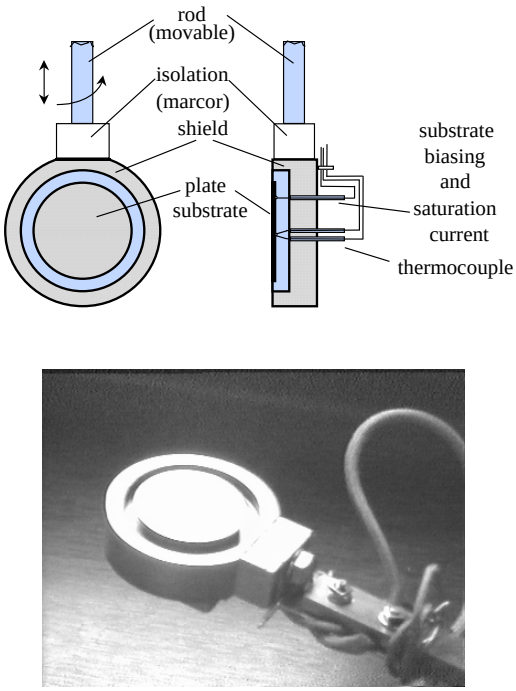

Fig. 1. A schematic sketch and a photograph of the thermal probe.

conduction to (or from, in case of a heated substrate) the substrate holder will be the dominant heat sink (source).

Energy flux measurements by a thermal probe: evaluation of the temporal slope of the substrate temperature

The integral energy influx from the plasma towards the substrate can be measured by a simple thermal probe [32]. Previously Thornton [33] and Wendt *et al.* [34] have proposed a similar procedure for the determination of the total heat influx. A schematic sketch of the setup is shown in Fig. 1. The probe is mounted on a manipulator arm to allow for horizontal and vertical scans. It can be also rotated, in order to measure directional fluxes, e.g. secondary electrons coming from an rf electrode or infrared photons from a heated surface.

In our experiments the heat flux measurements are carried out by observing the rate of temperature rise $\mathrm{d}T_S/dt$ of a metal substrate which is spot-welded to a thermocouple (type j) and placed within a solid shield. The substrate is only connected to the thermocouple and a wire for additional biasing. No other contact to the shield and holder is realized in order to minimize thermal conduction. Because of its large heat capacity the shield is at a constant environmental temperature T_{env} during the time of the measurement.

The measurement of the total energy influx Q_{in} is based on the determination of the difference between the time derivatives of the substrate temperature T_S during heating ("plasma on")

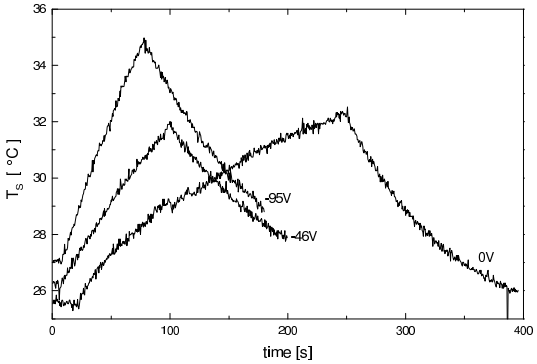

Fig. 2. T_S(t)-curves as measured during the Ar plasma process ($p = 1$ Pa, $P = 15$ W) for three substrate voltages (0, -46, -95 V).

and cooling ("plasma off"). Examples of typical temperature curves $T_S(t)$ which have been obtained for an Ar plasma ($p = 1$ Pa, $P = 15$ W) at three different substrate voltages are presented in Fig. 2.

The general power balance at the substrate is given by Eq. (11). The losses are always small in comparison to the incoming fluxes due to the plasma process. During the heating phase ("plasma on": $Q_{in} > 0$) H_S is determined by $\dot{H}_S(\text{heat}) = Q_{in} - Q_{out}$ and during the cooling phase ("plasma off": Q_{in}=0) by $\dot{H}_S(\text{cool}) = -Q_{out}$. By taking these expressions into Eq. (11) the difference yields the energy influx:

$$Q_{in} = \dot{H}_S(\text{heat}) - \dot{H}_S(\text{cool}) = -mc \left[\left(\frac{dT_S}{dt} \right)_{heat} - \left(\frac{dT_S}{dt} \right)_{cool} \right]_T . \tag{12}$$

If the slopes dT_S/dt are determined at the same temperature T and assuming no change of the environmental temperature T_{env}, which is achieved by short measurement times, the expression within the brackets of Eq. (12) is a quantity proportional to the thermal power at the substrate. In order to obtain absolute values of Q_{in} the specific heat of the substrate (thermal probe) has to be determined by a known thermal power as described in [35].

The measured energy influx is an integral value comprising the various contributions as kinetic energy of charge carriers, recombination heat, reaction heat, etc. By measuring the energy fluxes at different substrate voltages V_S , the contributions of ions and electrons from the other sources can be separated. For this purpose, the thermal probe (substrate) can be biased externally by a dc voltage. Simultaneously, the electrical current to the substrate is measured and one obtains the substrate characteristic, which is similar to a usual probe characteristic. In Fig. 3 the thermal probe characteristic in an 1 Pa argon and oxygen rf plasma is shown. At sufficiently negative substrate voltages the current I_S changes only slightly with increasing voltage V_S. From the characteristics in Fig. 3 an ion saturation current of about 1 mA and a floating potential of $V_{fl} \approx -3$V can be obtained for the argon plasma.

Determination of the energy influx by measuring the temperature gradient

In comparison to the described temperature rise method there is another simple and reliable procedure to measure the heat influx at the substrate by determination of the temperature gradient

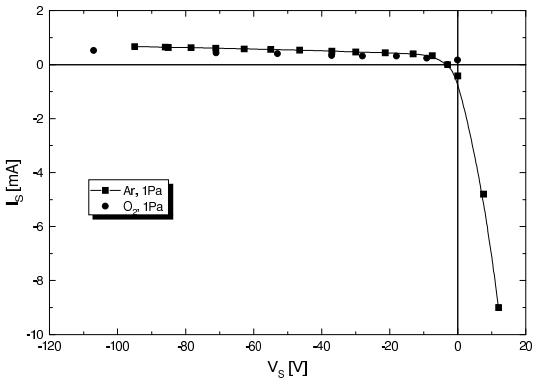

Fig. 3. Current-voltage characteristic of the substrate (thermal probe) for argon and oxygen.

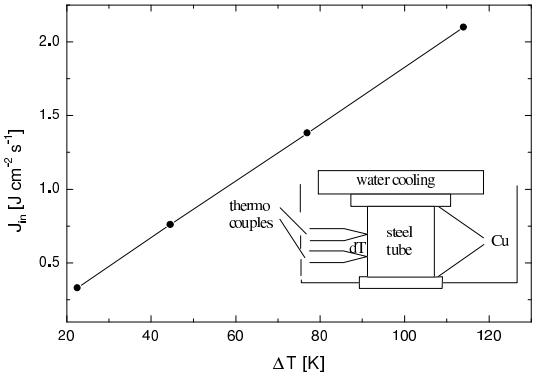

Fig. 4. Calibration: integral energy influx vs. Measured temperature difference between two thermocouples, from [17].

along the sample holder [17]. At this method the power flux is measured in steady state:

$$\text{const} \times Q_{in} \approx \frac{\Delta T}{\Delta x}. \tag{13}$$

The heat capacity of the device should be relatively small and the distance between the thermocouples can be enlarged by using a tube between substrate and water cooling (see Fig. 4). The calibration of the differential expression $\Delta T / \Delta x$ can be done by means of an electrical heater of known power. Thus, by using such a calibration the integral influx can be determined from the measured temperature gradient along the substrate holder tube.

Energy flux measurements by fluorescent powder particles

A rather new method for the determination of energy fluxes in a process plasma on the basis of the thermal balance of injected powders has been recently performed by Swinkels *et al.* [36]. In order to monitor the temperature T_p of the powder particles, which is a result of the different energy fluxes towards and back from them, fluorescence measurements have been carried out.

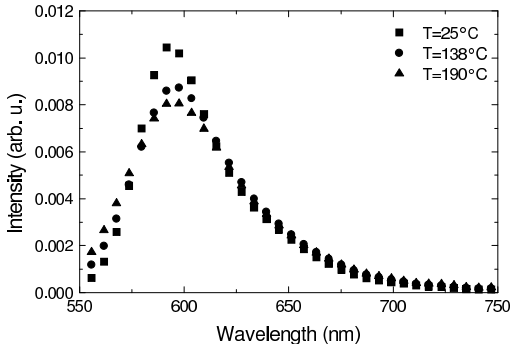

Fig. 5. The spectral profile of MF/RhB fluorescent emission curves for three different temperatures. The dye incorporated into the MF spheres is excited with an argon ion laser operating at 514 nm and 28 mW.

The particles are melamine-formaldehyde (MF) spheres, which are dyed throughout the volume with Rhodamine B (RhB). An argon ion laser was used to excite the dyed particles. The resulting fluorescent emission has been recorded using an optical multi-channel analyzer. In Fig. 5 a few calibration curves of the particle temperature are shown for the MF/RhB particles. The calibration curves show that the spectral profile of the fluorescent emission depends on the temperature. One can clearly see that as function of temperature the curve broadens and the intensity decreases. This makes it possible to determine the particle temperature T_p in plasmas without making use of the absolute intensity. During the plasma process the powder particles undergo a thermal power balance which takes into account the several energy fluxes arriving at and leaving from the particle surface as kinetic energy of electrons and ions, ion recombination energy, thermal conduction, and radiation. Measurement of the internal particle temperature T_p yields valuable information about these different fluxes.

In the stationary case where the particles, which float near the plasma sheath edge, are heated to their equilibrium temperature T_p the energy fluxes are equal: $Q_{in} = Q_{out}$. Hence, by knowledge of the outgoing flux Q_{out} which consists of the thermal conduction and the radiation the total energy flux towards a powder particle can be obtained and compared with model calculations for Q_{in}. The loss terms are essentially determined by the particle temperature T_p and the gas temperature T_g which have been measured by the fluorescence of the particles dye and absorption profiles, respectively.

4 Experimental examples for energy balances during plasma processing

Low temperature plasma processing of solid surfaces is essentially affected by energetic and thermal quantities, as energy per incoming particle (E), particle flux (j), energy flux density (energy dose, ($J = jE$) from the plasma and electrodes, and substrate temperature (T_S). In the following we will illustrate the influence of the different energetic and thermal quantities at some experimental examples of thin film deposition.

A characteristic feature of thin film deposition by magnetron sputtering in comparison to thermal evaporation is the higher kinetic energy of the particles arriving at the substrate. The integral energy influx (Q_{in}) during sputtering influences the thermal conditions at the substrate surface

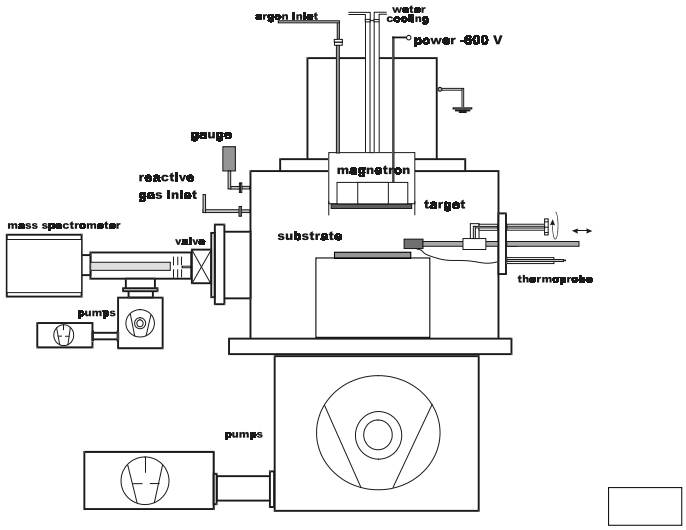

Fig. 6. Schematic of the experimental set-up for sputtering of a-C:H-films and molybdenum thin films.

and, hence, in addition to momentum transfer it effects the microstructure and morphology as well as adhesion and residual stress of the deposited films [1,13].

4.1 Magnetron sputtering of carbon films

The energy influx Q_{in} (deposited power) during thin film deposition by sputtering of a graphite or molybdenum target, respectively, in an Ar/H_2 (1.5:1) atmosphere has been measured as a function of the magnetron discharge power, gas pressure, and radial position beneath the target. The magnetron set-up is shown in Fig. 6, and the experimental details have been described elsewhere [37]. Opposite to the planar target cathode (diameter: 90 mm) the radially movable thermal probe was placed in a distance of 45 mm which is the typical distance of the normally used substrates. The target voltage has been varied in the range of 350 ... 550 V corresponding to a discharge power of 10 ... 150 W and the gas pressure (argon and/or hydrogen) could be varied between 0.5 ... 5 Pa. For the calculation of the several contributions to the total energy influx the internal plasma process parameter have to be known. Therefore, the electron density n_e, the electron temperature kT_e as well as floating and plasma potential (V_{fl}, V_{pl}) in the substrate region have been determined by Langmuir-probe measurements. The temporal behaviour of the discharge, the gas composition, and the target oxidation state has been monitored by mass spectrometry. TRIM calculations [38] were used to obtain the energy of the sputtered and reflected particles arriving from the target to the substrate.

In order to obtain absolute values of Q_{in} the specific heat of the substrates (thermal probe) were determined by a known thermal power from cw laser irradiation and as described in [39]. It was $C_s = mc = 0.6$ J/K for a copper plate as shown in Fig. 1.

As an example, in Fig. 7 the energy influx versus power is plotted for different experi-

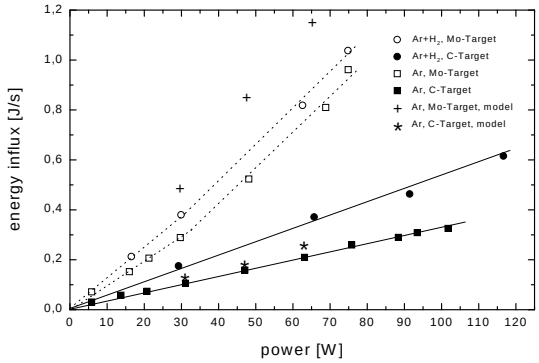

Fig. 7. Energy influx as measured for C-sputtering and Mo-sputtering, respectively, in Ar and Ar/H_2 in dependence on the supplied magnetron power ($p = 1.5$ Pa). The measurements are compared with calculated values based on a balance of the different energetic contributions.

mental conditions. First, we will briefly discuss the curves for the graphite target: For a constant gas pressure Q_{in} rises linearly with increasing discharge power in both cases, in Ar as well as in Ar/H_2. This is due to the increasing charge carrier density in the substrate region ($n_e = 5 \times 10^8 \ldots 2 \times 10^9$ cm^{-3}) and an increasing deposition rate of the condensing film ($R_{dep} = 0.1...0.5$ nm/s). By taking into account the heat of condensation ($q_c = 2.7 \times 10^7$ J/kg) and the layer density ($\rho = 2.0 \ldots 3.2$ gcm^{-3}) which has been determined by XRD the contribution of the condensation Q_C could be obtained by

$$Q_C = q_C \, \rho R_{dep} A, \tag{14}$$

where $A = 9$ cm^2 is the area of the thermal probe. The energetic contributions of the ions (Q_i) and electrons (Q_e) and for their recombination (Q_{rec}) can be specified as mentioned above by [40]:

$$Q_i = n_e \sqrt{\frac{kT_e}{m_i}} \exp(-0.5) e_0 V_{bias} A, \tag{15}$$

$$Q_e = n_e \sqrt{\frac{kT_e}{2\pi m_e}} \exp\left(-\frac{e_0 V_{bias}}{kT_e}\right) 2kT_e A, \tag{16}$$

$$Q_{rec} = j_i (E_i - \Phi) A \tag{17}$$

(m_e, m_i: mass of electrons and ions, j_i: ion flux density, E_i: ionization potential, Φ: work function, $V_{bias} = V_{pl} - V_S = 10 \ldots 15$ V and $V_S = V_{fl}$).

In the case of carbon sputtering in a pure argon plasma only the contributions listed above will influence the thermal balance of the substrate surface. Hence, the sum $Q_{in} = Q_C + Q_i + Q_e + Q_{rec}$ will result in the total energy influx measured by the thermal probe. The stars in Fig. 7 indicate the model calculation on the basis of Eq. (14) - Eq. (17) where the plasma parameters which are necessary for the calculations have been obtained by the diagnostics as described above.

If hydrogen is added during the sputtering process the thermal load is remarkably higher than for pure argon sputtering. This is due to an additional energetic contribution due to the

recombination of hydrogen atoms on the surface of the thermal probe. The influence of hydrogen could also be observed in the dependence of Q_{in} on the pressure. Whereas the energy influx for a constant discharge power increases slightly with the pressure in the case of sputtering in pure argon, it decreases with increasing pressure for the Ar/H_2 mixture. This observation might be explained by two facts: Firstly, at higher gas pressure the hydrogen recombination becomes more likely in the volume than at the surface and, secondly, a higher hydrogen supply at the substrate results also in enhanced reactions of C_xH_y compounds which "consume" energy.

The results for sputter deposition of molybdenum show the same qualitative behavior. However, the energy input is essentially higher than for the graphite target. Because of the smaller thickness of the Mo target the bonding to the magnetron water cooling was very poor and, hence, the temperature of the Mo target reached values up to 400 - 900 K depending on the discharge power, while the C target temperature was only in the range of 320 - 400 K. Thus, in the case of Mo sputtering the heat radiation from the target delivers a large contribution to the total energy balance of the substrate. For molybdenum also the influence of the kinetic energy of the sputtered atoms (Q_n) arriving at the substrate have to be considered which is cannot be neglected as in the case of carbon sputtering:

$$Q_n = R_{dep}\frac{N_A\rho}{M}E_n \tag{18}$$

(atomic mass of Mo: M=96, N_A: Avogadro's number, $\rho < 10.2$ g/cm^3: Mo film density). The mean energy E_n of the sputtered Mo atoms has been calculated by TRIM to be in the order of $E_n = 3.3$ eV for our experimental conditions. By taking into account these effect the energy influx has been calculated again, the results are indicated by the crosses in Fig. 7.

4.2 Influence of energetic contributions during DC-magnetronsputtering of aluminum films on microstructure

In the following example of aluminum sputtering (Fig. 8), the measured total energy influx, which has been determined again from the rise of the substrate temperature (dT_S/dt) during the sputtering process, consists mainly of the kinetic energy of charge carriers and sputtered particles, and the released condensation heat [41].

The contribution of ions (J_i) and electrons (J_e) could be distinguished again by variation of the substrate potential. The effect of sputtered particles on the energy balance ($J_{n,sput}$) is estimated by the product of their flux density and the mean kinetic energy which has been determined from the energy distribution of sputtered species. Finally, the contribution J_c due to condensation of aluminum particles has been determined by measuring the deposition rate and by taking into account of the specific condensation heat.

The Al films were sputtered by a DC magnetron onto glass or silicon substrates or onto microdisperse powder particles, respectively. The discharge voltage was operated at 250 ... 550 V and the current range was 20 ... 250 mA. Standard argon gas pressure was 0.01 mbar at a gas flow rate of 50 sccm. The distance between target and substrate could be varied between 4 and 15 cm. Opposite to the magnetron, at the bottom of the reactor an RF electrode was installed, which was necessary for charging and trapping of injected powder particles in order to modify them [42]. The discharge has been studied by several diagnostics. Langmuir-probe measurements and self-excited electron resonance spectroscopy (SEERS) [43] provided information on

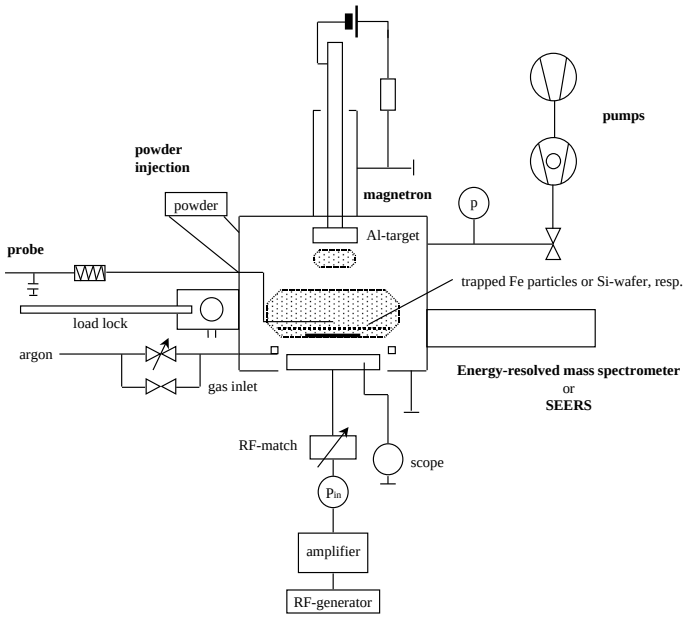

Fig. 8. A schematic view of the experimental set-up for aluminium sputtering onto flat substrates and powder particles.

the electrons whereas the ion and neutral component was monitored by energy resolved mass spectrometry. The deposited films were investigated by analytical techniques as scanning electron microscopy (SEM), X-ray- photoelectron spectroscopy (XPS), Rutherford backscattering (RBS), and atomic force microscopy (AFM).

In the present study the internal plasma parameters as V_{pl}, V_{fl}, n_e, kT_e etc. have been measured in the substrate region which is relevant for the fluxes to the substrate. The measurements of the plasma parameters have been carried out for only the RF discharge as well as for the combined operation of RF plasma and DC magnetron as it was commonly used in powder treatment. Of course, in magnetron operation the plasma parameters in comparison to the weak RF discharge are remarkably changed.

From the number of ions arriving at the target and their mean energy the yield and, hence, the flux of sputtered Al particles (j_{Al}) to the substrate has been estimated using TRIM to be in the order of a few 10^{16} cm^{-2}s^{-1} for our experimental conditions. Supposing that all sputtered Al atoms which strike the substrate are also stick on it, one can simply calculate the growth rate. The calculated Al deposition rate R_{dep} is in quite good accordance with the rates measured by RBS and optical transmission, respectively, as it can be seen in Fig. 9. The energy influx to the substrate and, consequently, the substrate heating during sputter deposition with a magnetron source is a combination of different heating contribution. As is the case for all vapour deposition processes, the heat of condensation (J_c) must be considered, which is for aluminum in the order of $q_c = 104$ kJ/kg (E_c=3.3 eV/atom). The contribution J_c to the energy influx due to film

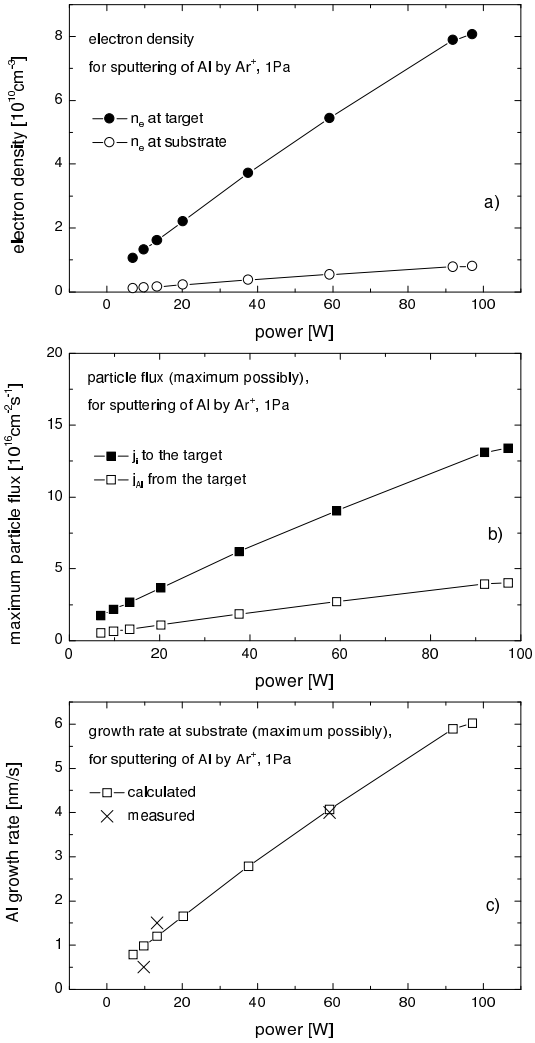

Fig. 9. Electron density (a), particle fluxes (b), and results of model calculation for Al growth compared with measured deposition rates vs. power (c).

condensation is corresponding to:

$$J_C = q_C \, \rho R_{dep} = j_{Al} E_C \tag{19}$$

(R_{dep}: deposition rate, ρ: mass density).

The contribution J_{ch} due to the kinetic energy of charge carriers (electrons and Ar ions) depends on the electron density in the substrate region and the mean kinetic energy of the carriers which is determined by the bias potential $V_{bias} = V_{pl} - V_S$. Because the substrates were always at floating potential, it is $V_S = V_{fl}$. The energetic contributions (J_e, J_i) of the charge carriers have been obtained according to Eqs. (15), (16).

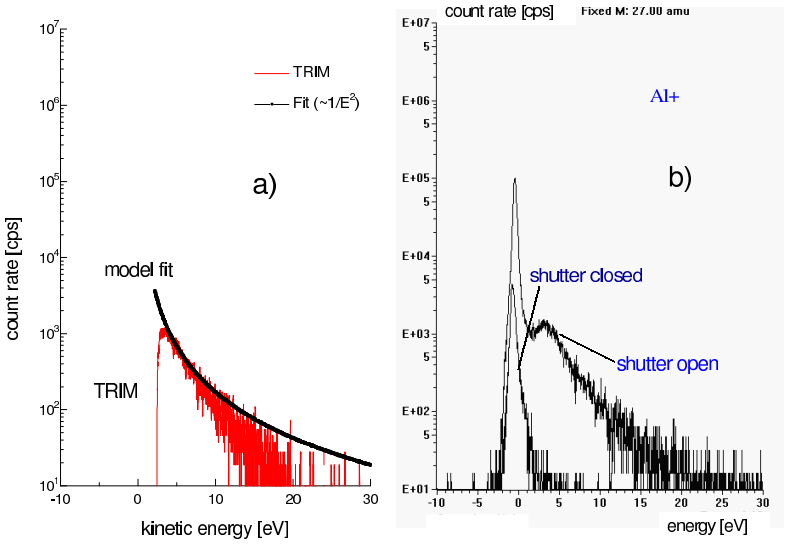

Fig. 10. Simulation (a) and measurement (b) of the energy distribution of sputtered aluminium for a discharge voltage of 440 V.

The electron energy was kT_e=4.2 eV and the electron density in the substrate region during sputtering was measured to be in the order of $n_e = 5 \times 10^8 \ldots 3 \times 10^9$ cm^{-3} depending on the discharge power. In case of floating substrates the released recombination energy flux J_{rec} has to be considered:

$$J_{rec} = j_i E_{rec}, \tag{20}$$

where $j_i = j_e$ and E_{rec} is the ionization energy, which is for argon 15.7 eV. Due to low operating pressure of the magnetron, a significant fraction of the kinetic energy E_n of the sputtered Al atoms may still be present for the depositing atoms in the substrate region. This contribution $J_{n,sput}$ is then:

$$J_{n,sput} = j_{Al} E_n = R_{dep} \frac{N_A \rho}{M} E_n. \tag{21}$$

The kinetic energy E_n of the sputtered neutrals has been calculated by TRIM for a magnetron discharge voltage of 440 V. The simulation yields a mean value of 2.9 eV/atom. In addition, the energy distribution of the sputtered species has been experimentally obtained by plasma monitor measurements (Fig. 10). In the measured spectra one can observe a peak due to the sputtered Al particles exactly at that position ($\sim$ 3 eV), which has also been obtained by TRIM simulation. The energy distribution of the sputtered aluminum particles decreases after its maximum accordingly to $\sim E_n^{-2}$ as expected from the theory [44,45].

The different contributions to the energy influx as described above are calculated for typical experimental conditions as used in magnetron sputtering and plotted versus the electron density in the substrate region in Fig. 11. Because the substrates are at floating potential, the energetic

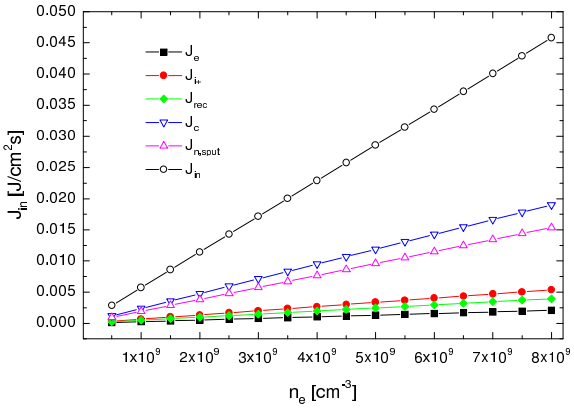

Fig. 11. Calculated contributions to the integral energy influx towards the substrate at magnetron sputtering ($V_S = V_{fl}, p = 1$ Pa).

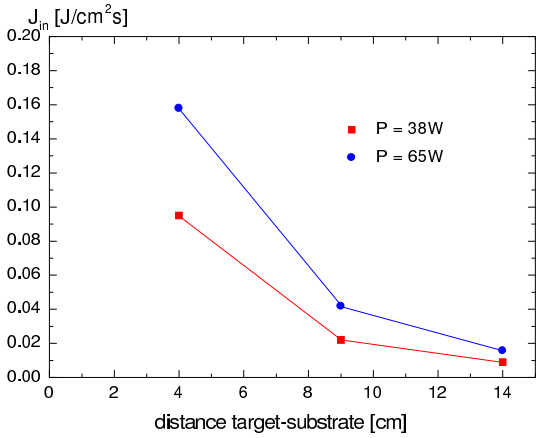

Fig. 12. Measured integral energy fluxes at magnetron sputtering of aluminium. The substrates were at floating potential.

contributions of the charge carriers in comparison to the kinetic energy of the sputtered particles and the condensation energy of the film are rather low.

The total energy influx J_{in} has not only been calculated, it has also been measured with thermocouples. From the temporal change of the substrate temperature the integral deposited energy has been obtained by the method as described above. The experimental results for J_{in} at various deposition conditions are plotted in Fig. 12. Comparison of measured and calculated values of J_{in} shows an excellent accordance. For instance, magnetron operation at 65 W and a target-substrate distance of 14 cm corresponds to an electron density in the substrate region of $n_e = 3 \times 10^9 \mathrm{cm}^{-3}$ and an aluminum growth rate of R_{dep} = 1.1 nm/s. Looking for the corresponding energy fluxes yield in each case 0.017 J/cm^{2}s.

Surprisingly, the films sputtered onto small iron powder particles exhibit a rough, cauliflower-like structure compared to the smooth layers sputtered onto flat silicon wafers. The difference is

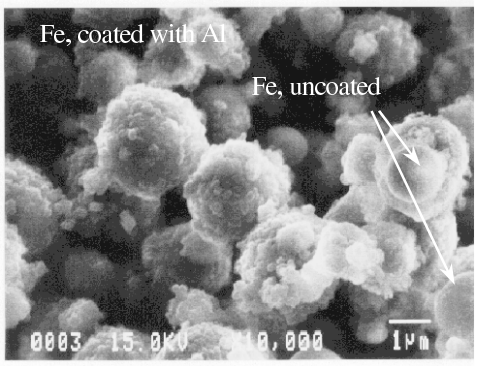

SEM picture of Al-coated Fe powder particles

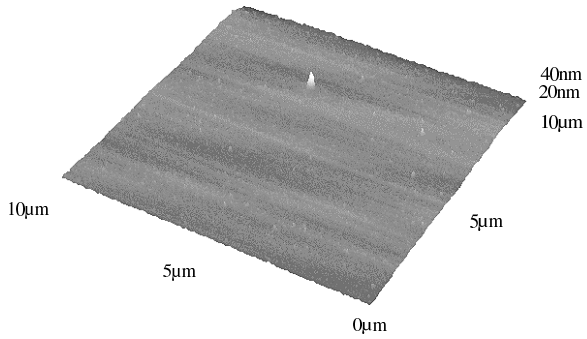

AFM picture of Al-coated Si substrate

Fig. 13. SEM micrograph of Al coated iron particles and reconstructed 3D-plot of a sputtered Al film on silicon as examined by AFM. Although the films have been sputtered under the same plasma conditions there is a remarkable difference in the microstructure.

obvious if one compares the SEM micrograph of coated powder particles with the AFM picture of the aluminum film on silicon in Fig. 13. An essential reason for the observed differences in surface roughness might be the different substrate temperature which is reached during the sputter process. Although under comparable deposition conditions the energy influx towards a powder particle is the same as towards a flat substrate, the resulting temperature may be quite different. Due to much better heat conduction along the substrate holder the silicon substrate do not reach such high equilibrium temperatures as microscopic powder particles, which are mainly cooled by radiation. Assuming an upper limit for the energy influx of 0.2 J/cm^{2}s which might be attained at high discharge power and low substrate-target distances the equilibrium temperature of a floating powder particle may reach values between 460 and 770 K. The first value is valid if one assumes a heat radiation emission coefficient of $\epsilon_S = 0.9$, while the latter has been obtained for $\epsilon_S = 0.1$. Especially for aluminum the effect of increasing grain size as the substrate temperature is increased, has been reported in literature [46].

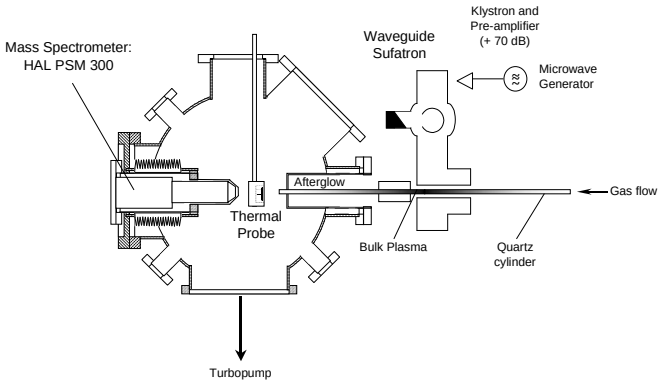

Fig. 14. Schematic of the experimental set-up for the thermal probe measurements in the remote plasma of a surface wave sustained discharge.

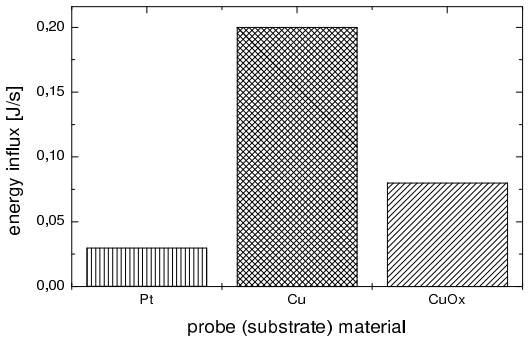

Fig. 15. Energy influx released by nitrogen recombination at different substrate materials in the afterglow of a surface wave sustained discharge.

4.3 Measurement of the energy influx released by atomic nirtogen recombination

In another experiment the energy input by recombination of nitrogen atoms in the afterglow of a surface-wave sustained plasma has been determined. In this experiment smaller thermal probes were used, and - in order to examine the influence of different surfaces on the recombination mechanism - in addition to the copper probe (C_S = 0.075 J/K) also probes of oxidized copper or platinum (C_S = 0.044 J/K), respectively, have been taken.

The plasma is created in a quartz tube by means of 2.45 GHz microwave power Klystron coupled to a Waveguide-Surfatron structure [47]. The system is fixed to a cylindrical reaction chamber (dimensions: 340 mm diameter, 590 mm high), see Fig. 14. The microwave discharge power in the discharge tube was varied between 200 W and 1000 W, as process gas pure nitrogen has been used at a pressure of 0.7 Pa in the chamber, where the afterglow expands into. In some experiments a N_2/O_2 mixture has been used in order to oxidize the copper probe. After such a measurement the oxide was removed by an argon beam. The thermal probe was placed immediately in front of the tube nozzle. Optical emission spectroscopy and mass spectrometry

have been performed as diagnostic tools in this experiment.

A quite large amount of the nitrogen molecules are dissociated in the bulk plasma of the tube and expand through the nozzle into the process chamber. The recombination of the N-atoms occurs at the substrate (probe) which is placed in front of the nozzle. Because the radiation and the charge carrier density in this region is negligible and no deposition takes place, the only contributions to the substrate heating are the gas temperature and the released recombination heat of the N_2 molecules:

$$Q_{in} \sim j_N \gamma_S E_{dis} \tag{22}$$

(E_{diss}: dissociation energy, γ_S: recombination probability, j_N: nitrogen atom flux density).

The influence of the recombination to the energy balance of the probe depends on the surface material (γ_S) on which the atoms recombine. Therefore, different substrate surfaces have been investigated: platinum, copper, and copper oxide.

The first preliminary results indicate clearly that under comparable experimental plasma conditions (power, pressure, atomic nitrogen flux) the energy influx for the different surface materials can be distinguished. As shown in Fig. 15 the recombination probability on copper is more than twice as much as for copper oxide, while the recombination on a platinum surface is even still lower. By a more quantitatively study which will take into consideration the precisely measured N- atom flux (j_N) it should be possible to re-calculate the energy released by a single nitrogen recombination ($\gamma_S E_{dis}$) on a special surface.

5 Summary

The energy influx towards the surface is one of the most important properties of plasma wall interaction for comparing and scaling-up several plasma processes. We have described how the various contributions to the energy balance of a plasma-exposed solid surface can be determined in general. By knowing the temporal and spatial evolution of the surface temperature and therefore of the thermal conditions at the solid surface during plasma treatment one can obtain information on the energy transfer mechanisms which are take place and which determine these thermal conditions.

Acknowledgements This study was supported by the Deutsche Forschungsgemeinschaft under SFB 198. The authors would like to thank J. Schulze, H. Steffen and G.H.P.M. Swinkels as well as Mrs. H. Boldt and A. Knuth for their support.

References

[1] J. A. Thornton: *J. Vac. Sci. Technol.* **11** (1974) 666

[2] B. Hussla, K. Enke, H. Grunwald, G. Lorenz, H. Stoll: *J. Phys. D, Appl. Phys.* **20** (1987) 889

[3] H. Deutsch, H. Kersten, A. Rutscher: *Contrib. Plasma Phys.* **29** (1989) 263

[4] H. Deutsch, H. Kersten, S. Klagge, A. Rutscher: *Contrib. Plasma Phys.* **28** (1988) 149

[5] J. L. Zubimendi, M. E. Vela, R. C. Salvarezza, C. Vazquez, J. Vara, A. J. Arvia: *Phys. Rev. E* **50** (1994) 1367

[6] S. D. Bernstein, T. Y. Wong, R. W. Tustison: *J. Vac. Sci. Technol. B* **12** (1994) 605

[7] S. Kugler, K. Shimakawa, T. Watanabe, K. Hayashi, I. Laszlo, R. Bellissent: *J.Non–Crystalline Solids* **164-166** (1993) 1143

[8] K. Bang, A. J. Ghajar, R. Komanduri: *Thin Solid Films* **238** (1994) 172
[9] H. Savaloni, M. A. Player, E. Gu, G. V. Marr: *Rev. Sci. Instrum.* **63** (1992) 1497
[10] H. Brune, H. Roder, K. Bromann, K. Kern: *Thin Solid Films* **264** (1995) 230
[11] H. Widischmann: *J. Appl. Phys.* **62** (1987) 1800
[12] S. M. Rossnagel: *Thin Solid Films* **171** (1989) 143
[13] K. H. Muller: *Appl. Phys. A* **40** (1986) 209
[14] R. Nimmagadda, R. F. Bunshah: *J. Vac. Sci. Technol.* **8** (1971) 677
[15] R. Chow, R. F. Bunshah: *J. Vac. Sci. Technol.* **8** (1971) 665
[16] J. A. Thornton: *Thin Solid Films* **54** (1978) 23
[17] H. Steffen, H. Kersten, H. Wulff: *J. Vac. Sci. Technol. A* **12** (1994) 2780
[18] H. Kersten, H. Steffen, D. Vender, H. E. Wagner: *Vacuum* **46** (1995) 305
[19] H. F. Winters, D. Horne: *Phys. Rev. B* **10** (1974) 55
[20] *Handbook of Chemistry and Physics*, CRC Press, 73rd edition, 1992/93
[21] H. Kersten, R. J. M. M. Snijkers, J. Schulze, G. M. W. Kroesen, H. Deutsch, F. J. deHoog: *Appl. Phys. Lett.* **64** (1994) 1496
[22] N. P. Tandian, E. Pfender: *Plasma Chem. and Plasma Proc.* **17** (1997) 353
[23] M. Tychi, P. Kundra, J. F. Behnke, C. Csambal, S. Klagge: *J. Phys. IV*, **7**, C3 (1997) 397
[24] F. Adler, H. Kersten, H. Steffen: *Contrib. Plasma Phys.* **35** (1995) 213
[25] D. E. Rapakoulias, D. E. Gerasimou: *J. Appl. Phys.* **62** (1987) 402
[26] M. Asscher, W. L. Guthrie, T. H. Lin, G. A. Somorjai: *J. Chem. Phys.* **78** (1983) 6992
[27] A. Durandet, O. Joubert, J. Pelletier, M. Pichot: *J. Appl. Phys.* **67** (1990) 3862
[28] H. Kersten, H. Deutsch, J. F. Behnke: *Vacuum* **48** (1997) 123
[29] H. P. Bonzel, R. Ku: *Surf. Sci.* **33** (1972) 91
[30] D. D. Deley: *Chem. Ind.* **1** (1976) 12
[31] J. A. G. Baggerman, R. J. Visser, E. J. H. Collart: in *Proceedings ISPC-11*, Loughborough, 1993, p.1410
[32] H. Kersten, E. Stoffels, W. W. Stoffels, M. Otte, C. Csambal, H. Deutsch, R. Hippler: *J. Appl. Phys.* **87** (2000) 3637
[33] J. A. Thornton: *Thin Solid Films* **54** (1978) 23
[34] R. Wendt, K. Ellmer, K. Wiesemann: *J. Appl. Phys.* **82** (1997) 2115
[35] H. Kersten, G. M. W. Kroesen, H. Deutsch, R. Hippler: submitted
[36] G. H. P. M. Swinkels, H. Kersten, H. Deutsch, G. M. W. Kroesen: *J. Appl. Phys.* **88** (2000) in print
[37] H. Kersten, D. Rohde, J. Berndt, H. Deutsch, R. Hippler: *Thin Solid Films*, to appear
[38] W. Eckstein, J. P. Biersack: *Z. Physik B* **63** (1986) 471
[39] XXXX
[40] D. Bohm: in *The characteristics of electrical discharges in magnetic fields*, edited by A. Guthrie and R. K. Wakerling, McGraw-Hill, New York, 1949
[41] H. Kersten, G. M. W. Kroesen, R. Hippler: *Thin Solid Films* **332** (1998) 282
[42] H. Kersten, P. Schmetz, G. M. W. Kroesen: *Surface and Coatings Technology* **108-109** (1998) 493
[43] M. Klick: *J. Appl. Phys.* **79** (1996) 3445
[44] J. Roth: in *Physics of plasma-wall interactions in controlled fusion, NATO ASI Series* **131**, edited by D. E. Post and R. Behrisch, p.351
[45] M. T. Robinson: *Phil. Mag.* **17** (1968) 639
[46] *Handbook of Thin Film Proc. Technol. (X2)*, edited by D. A. Glocker and S. I. Shah, IOP, 1995
[47] D. Douai, J. Berndt, J. Winter: in *Proceedings ISPC-14*, Praha, 1999